Modeling maps by using rational functions

O. Ménard, C. Letellier, J. Maquet, and G. Gouesbet
CORIA UMR 6614, Université et INSA de Rouen, Place Emile Blondel, 76821 Mont Saint-Aignan Cedex, France
(Received 24 September 1999; revised manuscript received 23 May 2000)

Rational functions are not very useful for obtaining global differential models because they involve poles that may eject the trajectory to infinity. In contrast, it is here shown that they allow one to significantly improve the quality of models for maps. In such a case, the presence of poles does not involve any numerical difficulty when the models are iterated. The models then take advantage of the ability of rational functions to capture complicated structures that may be generated by maps. The method is applied to experimental data from copper electrodissolution.

PACS number(s): 05.45.−a, 02.70.−c, 82.20.Wt

I. INTRODUCTION

A good understanding of a physical process generated by a dynamical system, in particular from the real world with a limited data set, requires a model. For the last decade, the idea that models may be extracted from time series without any prior knowledge of the underlying processes has been developed and good models have been obtained by using global modeling techniques applied to experimental data ([1–3], among others). There, it is assumed that the recorded variables have been produced by a deterministic dynamical system in the presence of noise. The aim is then to extract a mathematical model reproducing the deterministic part of the underlying dynamics. Furthermore, we focus on the case when the system is low dimensional, here meaning that it involves fewer than about ten variables. For a time-continuous behavior, the evolution of the system is described by a set of ordinary differential equations having the form $\dot{\mathbf{x}}=\mathbf{F}(\mathbf{x})$. In the case of a discrete-time behavior, the evolution is specified by a difference equation $\mathbf{x}_{n+1}=\mathbf{G}(\mathbf{x}_n)$, where n denotes time steps. Techniques devoted to the extraction of a model from a time series generated by a set of ordinary differential equations are called flow modeling techniques, whereas map modeling designates the case when a time series is generated by difference equations (in previous papers, the terminology of global vector field reconstruction has been used).

Although flow modelings have been extensively studied [2–7], map modelings are scarcer [1,4,8]. This fact is somewhat surprising, in so far as, in many situations, time series are actually generated by difference equations. Moreover, in the case of time-continuous systems such as the most studied Rössler and Lorenz systems, the associated equations for return maps are not known *a priori*. In such a case, successful map modelings can provide analytic information that cannot be otherwise analytically derived from the original differential equations. The extraction of such analytical information may be an important issue when the system is low dissipative, because knowledge of the equations for the Poincaré maps may allow one to determine the generating partition to encode chaotic trajectories [9].

Explicitly, Crutchfield and McNamara [1] obtained models for the Poincaré map generated by an experimental modified Van der Pol oscillator and for two data sets from a chaotic dripping faucet, by using polynomials as basis functions. Breeden and Hübler [8] investigated the case when a two-dimensional (2D) time series is generated by two coupled logistic maps. This is a very favorable situation because the functions to be approximated are then indeed polynomials, i.e., they possess the same structure as the basis functions with which they are approximated. A more difficult case is discussed by Giona, Lentini, and Cimagalli [4], who consider the Ikeda map [10], which constitutes a nonpolynomial system, for which, however, they obtained a satisfactory polynomial model from a 2D time series.

All the aforementioned map models are obtained by using polynomial expansions, i.e., smooth basis functions. One may note, however, that such functions are not necessarily appropriate to model a dynamics with apparent or real discontinuities, as observed on a four-branch first-return map from the Rössler system or from the Lorenz map. This is likely the reason why no difference equations have been proposed to model these maps. In this paper, we therefore propose to build map models by using rational functions that provide optimal fits for such maps. We shall also investigate a first-return map for experimental data from copper electrodissolution. The models will be validated by investigating their associated populations of periodic orbits through a probability density function of visits that is very efficient for validating the discrete models.

The paper is organized as follows. Section II is devoted to a mathematical background concerning the map modeling technique. In Sec. III, which is the main part of the paper, applications to numerical and experimental test cases are discussed. Section IV is a conclusion.

II. MAP MODELING TECHNIQUE

We consider maps reading as

$$\mathbf{X}_{n+1}=\mathbf{G}(\mathbf{X}_n), \tag{1}$$

where $\mathbf{X}_{n+1}$ is the state vector at the $(n+1)$th iteration ($n=0,1,\ldots$) and $\mathbf{G}$ defines the map under study. For an m-dimensional state vector, the system (1) involves m functions G_i which are, in principle, assumed to be unknown. The aim is thereafter to obtain approximations $\tilde{G}_i$ to the

functions G_i, starting from a time series made of consecutive values of one of the variables spanning the map. Let x_n designate this variable.

The problem of approximating functions starting from a time series, with a basis of polynomials, has already been considered in the case of flow modeling [1,2,4–6]. The approximation is then obtained by using a least-squares method to minimize a quadratic error function which compares actual values of the function and approximated values. Also, the functions are approximated by using multivariate monomial expansions on nets [6,11]. Similarly, in the case of map modeling, the functions G_i may be approximated by using polynomials. The approximation $\tilde{G}_i$ to G_i then reads as

$$\tilde{G}_i = \sum_{j=1}^{N_K} K_{ij} P^j \tag{2}$$

where P^j are monomials reading as, in the three-dimensional case,

$$P^j = x^k y^l z^m$$

with a biunivocal relationship between integers j and triplets (k,l,m) as defined in Ref. [6] and N_K the number of monomials retained in the approximation. Unfortunately, maps have very rarely been found to be well approximated by such polynomial approximations. Instead, rational functions are required to capture stiff variations observed on maps such as the Lorenz map or the four-branch Rössler map investigated in the next section. The functions G_i are then approximated as

$$\tilde{G}_i = \frac{\Sigma_{j=1}^{N_K^N} N_{ij} P^j}{\Sigma_{j=1}^{N_K^D} D_{ij} P^j}, \tag{3}$$

where N_K^N is the number of monomials retained in the numerator and N_K^D is the number of monomials retained in the denominator. The coefficients N_{ij} and D_{ij} can then be determined according to $x_{i,n+1} = \tilde{G}_i(x_n, y_n, z_n)$, which may be rewritten as

$$x_{i,n+1}\left(\sum_{j=1}^{N_K^D} D_{ij} P_n^j\right) = \sum_{j=1}^{N_K^N} N_{ij} P_n^j \tag{4}$$

in which x_i is x, y, or z for $i=1$, 2, or 3, and P_n^j is P^j at time step n. Equation (4) defines an approximation problem which can be solved by using N_v vectors $X_n = (x_n, y_n, z_n)$ with $N_v \geqslant (N_K^N + N_K^D)$. Nevertheless, one of the denominator coefficients must be assigned a value to avoid a degeneracy problem [5]. We arbitrarily set $D_{i1} = 1$. The number of retained vectors for solving the problem must therefore now satisfy the condition $N_v \geqslant (N_K^N + N_K^D - 1)$ and

$$\sum_{j=1}^{N_K^N} N_{ij} P_n^j - x_{i,n+1}\left(\sum_{j=2}^{N_K^D} D_{ij} P_n^j\right) = x_{i,n+1} D_{i1}. \tag{5}$$

We have then to solve a system, constituted by N_v equations, taking the form

$$A \cdot K = B \tag{6}$$

in which A is an $N_v \times (N_K^N + N_K^D - 1)$ matrix and K is an $(N_K^N + N_K^D - 1)$-dimensional column vector, listing the unknown coefficients. Also, B is an N_v-dimensional column vector.

Equation (6) is solved by using a singular value decomposition of the A matrix [12], and the approximation is achieved by minimizing a quadratic norm:

$$L_2 = \sqrt{(AK-B)^\dagger (AK-B)} \tag{7}$$

where $(\cdot)^\dagger$ denotes the transposed matrix.

The quality of the model depends on the modeling parameters, which are N_v, the number of state vectors taken into account to approximate the functions; N_K^N, the number of coefficients in the numerator; and N_K^D, the number of coefficients in the denominator. The models will be validated by using a probability density function of visits as discussed in [13]. It must be noted that, although rational functions are no longer considered when a flow modeling is attempted, we will exemplify that, in the case where discrete maps are under consideration, rational functions allow us to increase significantly the class of maps that can be modeled. In such cases, there is no numerical problem during the iteration of the discrete models as encountered when flows are considered. Indeed, when a flow modeling is attempted with rational functions, the existence of singularities very often generates regions of the phase portrait where the trajectory is ejected to infinity. Although such regions represent a subset of the attractor of measure zero, they usually cannot be numerically avoided by the trajectory when a continuous model is searched. In contrast, when a discrete model is attempted, it concerns a Poincaré section (or a first-return map) which is generically chosen in a region of the attractor far from singularities.

III. APPLICATIONS

A. Numerical test cases

1. Ikeda map

In the simple cases where the maps are polynomial functions, like the logistic map or the Hénon map, the exact functions G_i are polynomials and, therefore, are easily matched by polynomial expansions for the approximated functions $\tilde{G}_i$. We are interested in investigating more complicated cases where such a structure matching does not occur. Our first example is the Ikeda map reading as [10]

$$\begin{aligned} x_{n+1} &= 1 + 0.7(x_n \cos \tau_n - y_n \sin \tau_n), \\ y_{n+1} &= 0.7(x_n \sin \tau_n + y_n \cos \tau_n), \end{aligned} \tag{8}$$

where

$$\tau_n = 0.4 - \frac{6.0}{1 + x_n^2 + y_n^2}. \tag{9}$$

As suggested by Giona, Lentini, and Cimagalli [4], this model is particularly interesting since it presents a nonpolynomial form although its behavior is quite simple as dis-

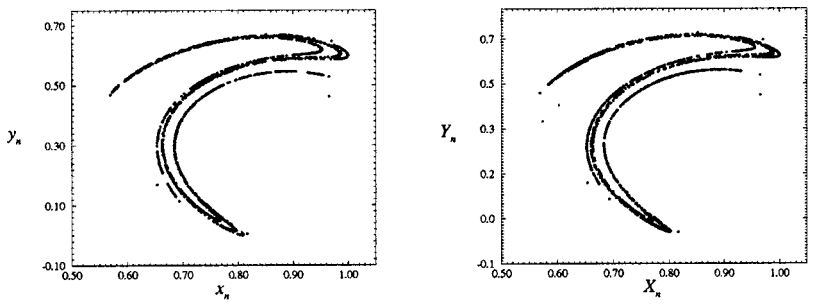

FIG. 1. The Ikeda map and its model obtained by using polynomial functions. Coordinates are normalized between 0 and 1.

played in Fig. 1(a). It therefore constitutes a good test case to exemplify the fact that nonpolynomial structures may be approximated well enough by using polynomial basis functions.

A rather good 2D model involving two functions has been obtained with polynomial structures by using the modeling parameters $(N_v, N_K) = (25,21)$ for the first function and $(N_v, N_K) = (22,21)$ for the second function. Increasing the number of retained vectors N_v or the number of monomials N_K does not help to obtain a better model. The model is displayed in Fig. 1(b). In order to check for the quality of the model, the invariant probability density function of visits [13] is used. It is computed from the x variable [Fig. 2(a)] for the original map. It may be favorably compared with the probability computed for the polynomial discrete model [Fig. 2(b)], although some amount of discrepancy can be visually observed.

The quality of the reconstruction may be quantitatively estimated by using a mean relative error averaged on small bins of the x coordinate used to build the histograms displayed in Figs. 2. This error is found to be equal to 2.3×10^{-3} and is drastically reduced to 10^{-5} by using more complex 2D models involving two rational functions. The best model, i.e., the one for which the error is the smallest, involving two rational functions is obtained with $(N_v, N_K^N, N_K^D) = (42,23,18)$ for the first function and $(N_v, N_K^N, N_K^D) = (50,20,29)$ for the second function. The invariant measure is displayed in Fig. 2(c). Indeed, the comparison between Figs. 2(a) and 2(c) is much better than between Figs. 2(a) and 2(b). If the number of terms in rational functions is increased, no better model, i.e., with a smaller error on the invariant density function, can be obtained. Moreover, increasing the statistics does not increase the quality of the model and may even decrease its quality by enlarging the numerical errors.

2. Lorenz map

A more acid test case is now investigated by considering the Lorenz map computed from the Lorenz equations for $R = 28.0$, $\sigma = 10.0$, and $b = \frac{8}{3}$ [14]. Although the time-continuous Lorenz system is indeed generated by polynomial functions, there is no known explicit form for the associated Lorenz map. This map is displayed in Fig. 3(a). A particular difficulty arises from the fact that this map exhibits a critical point, a cusp, where there is an actual derivative discontinuity. All trials with polynomial expansions failed, as expected, since it is rather difficult to fit such a discontinuity with (smooth) polynomial functions.

A map modeling is thereafter attempted by using rational functions. Of course, instead of rational functions, we could rather use piecewise polynomial functions. Nevertheless, such a piecewise model cannot be considered as a global model for the map. A 1D discrete model has been obtained with modeling parameters (N_v, N_K^N, N_K^D) equal to (51,22,23), i.e., the model has the form of Eq. (3). As an example, its coefficients are reported in Table I. The result of its integration is displayed in Fig. 3(b). Although very slight departures may be observed, the discontinuity associated with the criti-

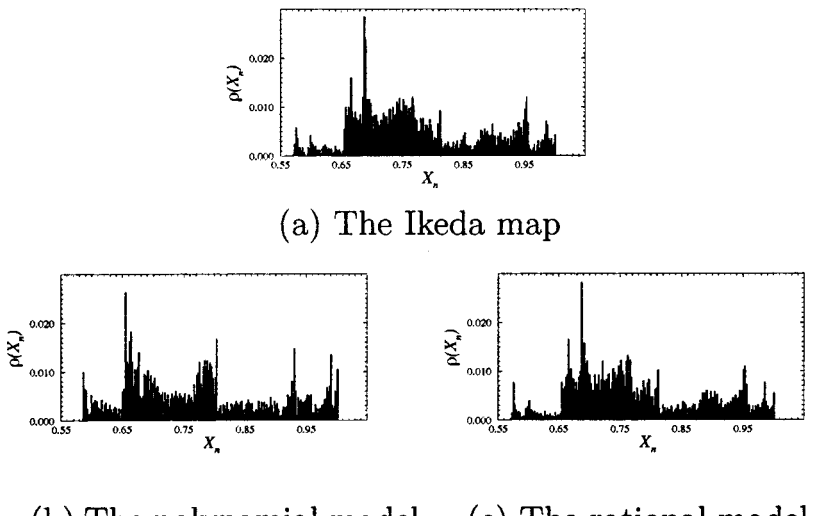

FIG. 2. Probability density functions of visits of the x coordinate for the original Ikeda map, a polynomial, and a rational model.

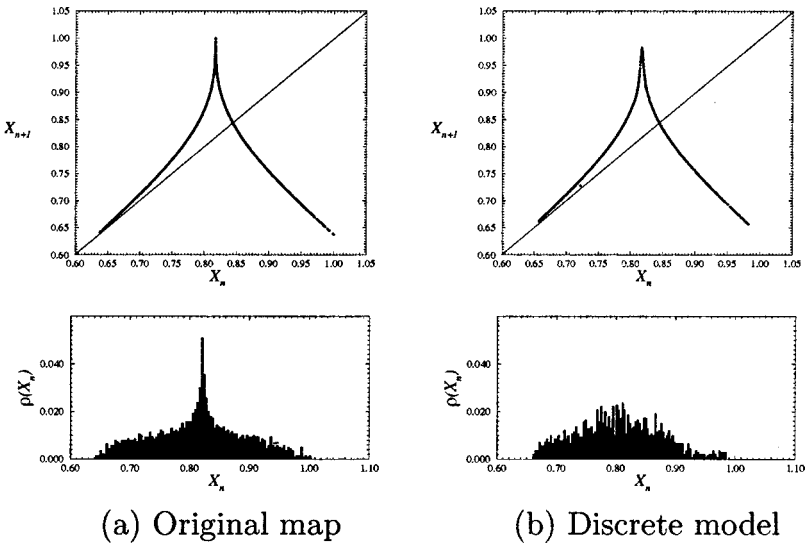

FIG. 3. Original map and model for the chaotic attractor generated by the Lorenz system ($R=28.0, \sigma=10.0, b=8/3$). Probability density functions of visits are also displayed.

cal point is quite well reproduced. The quality of the model is checked by computing probability density functions of visits (Fig. 3). The peak located at the cusp for the original map is not clearly recovered for the discrete model. This means that the cusp is not fully captured by the model. Nevertheless, the population of periodic orbits is only affected by such a discrepancy in terms of orbits whose period is greater than 6. No global model has been reported for this map before.

3. Rössler map

Another well known system is the Rössler system [15]. This system has three control parameters (a,b,c). When they are fixed to (0.398,2.0,4.0), the system generates a chaotic attractor that is characterized by a unimodal map. There is no known equation for this map. In this case, however, a model is easily found by using a polynomial expansion with modeling parameters $(N_v, N_K)=(5,5)$, i.e., only five points have been used for the approximation, corresponding to the lowest theoretical limit for which a model with five coefficients may be obtained. Such a feature is a signature of a very easy modeling. The model reads as

$$x_{n+1}=K_1+K_2x_n+K_3x_n^2+K_4x_n^3+K_5x_n^4 \tag{10}$$

with

$$K_1=-0.621\,249\,046\,487\,11,$$

$$K_2=1.161\,148\,250\,389\,67,$$

$$K_3=-0.749\,571\,054\,812\,79,$$

$$K_4=-0.563\,853\,804\,997\,65,$$

$$K_5=-0.060\,982\,181\,074\,680.$$

A more interesting case arises for $(a,b,c)=(0.523,2.0,4.0)$. The system then generates a chaotic attractor whose first-return map is constituted by four monotonic branches [16]. This map is displayed in Fig. 4(a). One may observe that there is a critical point (the minimal one) which is stiff. This may be the reason why no successful model has been obtained with a polynomial expansion. Nevertheless, a satisfactory 2D model of the form

$$x_{n+1}=G(x_n,y_n),$$

$$y_{n+1}=x_n \tag{11}$$

is obtained with modeling parameters for G given by $(N_v, N_K^N, N_K^D)=(34,9,11)$. The model is constituted by a single rational function in which two delay coordinates

TABLE I. Coefficients of the reconstructed map of the Lorenz map.

p	x_n power	N_p	D_p
1	0	0.089 388 145 015 673	1.000 000 000 000 0
2	1	−0.271 252 425 112 75	−8.591 434 992 786 3
3	2	−1.157 002 572 891 3	29.143 906 046 454
4	3	6.338 808 809 966 8	−45.778 835 787 513
5	4	−8.503 036 536 959 1	22.902 918 693 639
6	5	−1.620 510 733 187 6	19.574 207 763 519
7	6	8.097 715 305 686 4	−13.050 493 866 068
8	7	4.806 371 418 319 2	−19.499 230 076 356
9	8	−7.411 649 042 682 2	3.276 317 745 544 1
10	9	−8.420 288 842 051 0	16.071 238 494 349
11	10	1.727 175 485 887 8	8.173 255 462 660 8
12	11	9.848 968 071 216 6	−7.575 456 626 388 7
13	12	5.573 285 051 003 7	−13.203 796 710 811
14	13	−4.743 844 627 850 9	−33.849 832 873 339
15	14	−10.346 295 209 344	8.7.290 166 313 545
16	15	−2.582 402 129 452 1	10.572 341 426 795
17	16	8.074 233 164 029 4	0.192 321 354 963 08
18	17	8.747 881 061 694 0	−10.628 324 838 265
19	18	−4.612 821 723 101 1	−7.199 847 517 402 9
20	19	−11.526 534 433 515	7.374 346 713 566 1
21	20	10.301 636 497 816	10.878 248 212 930
22	21	−2.409 814 1903 439	−12. 350 247 547 655
23	22		3.374 549 281 351 1

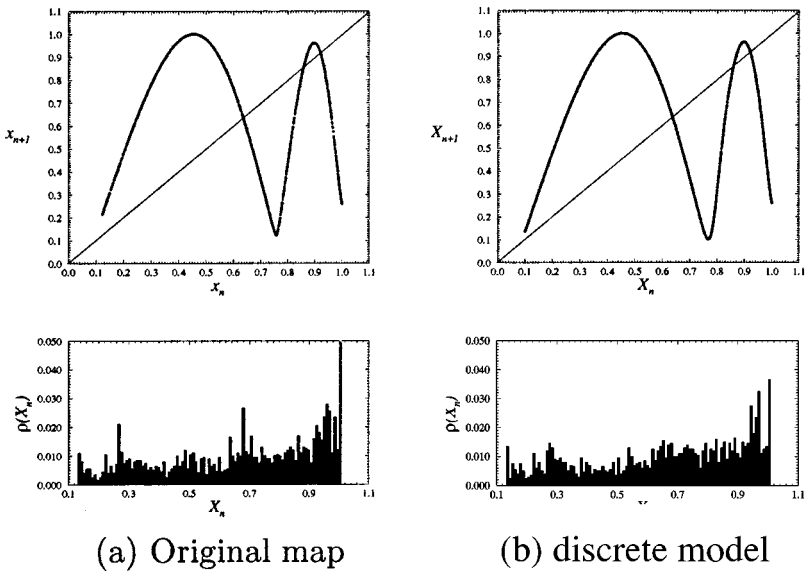

FIG. 4. Original map and discrete model for the chaotic attractor generated by the Rössler system ($a=0.523$, $b=2.0$, $c=4.0$). Probability density function of visits is also reported.

(x_n, x_{n-1}) are involved. An iteration of this model generates the map displayed in Fig. 4(b).

B. Experimental data

In this section we are interested in modeling the underlying dynamics governing an experimental data set described in terms of discrete maps. In order to do so, we use a data set extracted from the experimental time series by computing a first-return map to a Poincaré section from the time evolution of the current passing through an electrode of a copper electrodissolution experiment. This example is discussed to provide evidence of the ability of the method to capture experimental dynamics.

Periodic and chaotic oscillations have been observed in a number of electrochemically reacting systems [17]. Copper electrodissolution in H_3PO_4 has been found to undergo Hopf bifurcation to oscillatory behavior followed by a period-doubling bifurcation cascade to simple chaos [18]. The time series is obtained by recording the dissolution current $I(t)$ during potentiostatic electrodissolution of a rotating Cu electrode in phosphoric acid. The experimental setup is described in [3]. Only the asymptotic behavior is studied. The embedding dimension has been estimated to be equal to 3. The phase portrait may therefore be exhibited in a measurement phase space spanned by derivative coordinates $(X=I(t), Y=\dot{I}(t), Z=\ddot{I}(t))$ with a plane projection displayed in Fig. 5(a). A first-return map from a Poincaré section to itself is found to be constituted by two monotonic branches clearly enough separated by a critical point at $Y_c=0.32$ [Fig. 5(b)]. The Poincaré section is defined as $P\equiv\{(Y,Z)\in\mathbb{R}^2 | X=43.7, Y>0\}$.

One may remark that the first-return map displayed in Fig. 5(b) exhibits a significant thickness that cannot be captured by a 1D discrete model. Indeed, a successful model has only been obtained with a 2D model with rational functions reading as

$$x_{n+1}=\frac{F_N(x_n,y_n)}{F_D(x_n,y_n)},$$

$$y_{n+1}=x_n. \tag{12}$$

A few modeling parameters may allow one to find a model generating a map close to the experimental first-return map. Depending on the number of points used for the estimation, the thickness of the first-return map generated by the model is more or less large. Such a dependence of the thickness of the first-return map has not been observed when flow modeling using derivative coordinates was considered. This could result from the large flexibility of rational functions, which can therefore capture some dynamical properties resulting from the interaction of noise with the dynamics. In-

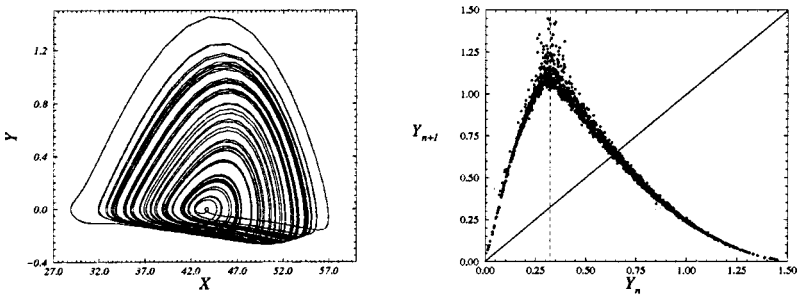

FIG. 5. Plane projection of the phase portrait reconstructed from the experimental data and a first-return map to the Poincaré section P.

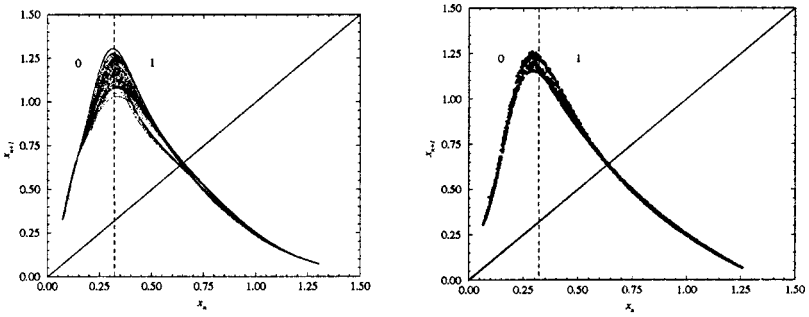

(a) $(N_v, N_K^N, N_K^D) = (22,5,14)$ (b) $(N_v, N_K^N, N_K^D) = (60,5,5)$

FIG. 6. Models for the first-return map from the data generated by copper electrodissolution.

deed, the action of noise may be compared, in a certain sense, to a reduction of the dissipation rate of a dynamical system. A larger structure, most often blurred, may then appear. While a rather thick model is obtained with the modeling parameters $(N_v, N_K^N, N_K^D) = (22,5,14)$, a thinner map is obtained when the number of points retained for the estimation is increased, i.e., $(N_v, N_K^N, N_K^D) = (60,5,5)$. Moreover, it may be remarked that the model computed on a larger set of points is constituted by a simpler rational function since the number of coefficients on the denominator N_K^D has been reduced from 14 to 5.

Using more points for the fit averages the influence of noise and allows one to obtain a better model from a dynamical point of view, and also better with respect to its complexity, since nine terms have been deleted. Increasing the number of retained points again does not improve the quality of this second model and even decreases it. Such a feature may result from two facts. First, when too many points are retained for estimating a model, the noise may be accumulated sufficiently to decrease the quality of the model. Second, when the length of the time series is increased, it may hapen that the trajectory visits for a long time the neighborhood of a periodic orbit which becomes preponderant in the statistics and, consequently, a model generating a limit cycle corresponding to the most visited periodic orbit is obtained.

The model may afterward be iterated to generate the model dynamical behavior (Fig. 6). One may observe that the model essentially captures the main features of the dynamics of the experimental map. Of course, the thickness of the discrete model is less significant than for the experimental data since a noise filtering process resulting from the statistics is involved.

The model cannot be validated by using the probability density function of visits because they are spoiled too much by noise contamination (but see Fig. 7). Nevertheless, symbolic planes (as defined in [3]) may be conveniently used as displayed in Fig. 7. They are found to be very similar although noise comtamination reveals itself by diffusing the structures of the experimental symbolic plane. As a consequence, since the noise is filtered in the modeling process, the model symbolic plane is less fuzzy. Let us mention, however, that the visual departures between symbolic planes are associated with a very small number of events. This is confirmed by the populations of periodic orbits, which are the same up to period 7 for the experimental and model data.

IV. CONCLUSION

Several models have been obtained for different kinds of nontrivial maps. We observed that modeling of discrete maps

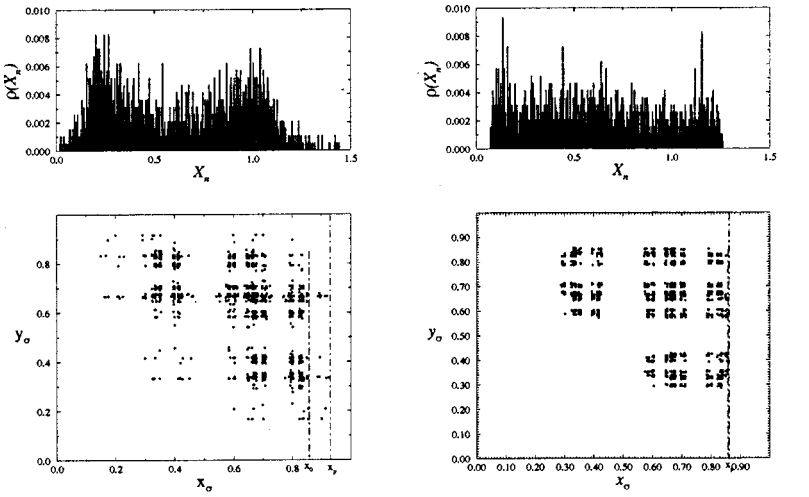

(a) Experimental map (b) Discrete model $(N_v, N_K^N, N_K^D) = (60,5,5)$

FIG. 7. Probability density functions of visits of the x_n coordinates and symbolic planes for the experimental map and the discrete model for copper electrodissolution.

may be improved by using rational functions. These functions enlarge the class of maps that may be successfully modeled. Such a result is particularly interesting since previous investigations have revealed that rational functions cannot be used for flow modeling without generating numerical difficulties when integrating the differential models. For map modeling, such difficulties are not encountered and, in particular, a successful map has been obtained to modelize the first-return map generated by copper electrodissolution. Consequently, if rational functions are not recommended for flows, they become very efficient for modeling discrete maps.

ACKNOWLEDGMENTS

We wish to thank Professor J. Hudson and Professor Z. Fei for their beautiful data generated for copper electrodissolution. O. Ménard is supported by the Région de Haute-Normandie.

[1] J. P. Crutchfield and B. S. McNamara, Complex Syst. **1**, 417 (1987).
[2] R. Brown, N. F. Rulkov, and E. R. Tracy, Phys. Rev. E **49**, 3784 (1994).
[3] C. Letellier, L. Le Sceller, P. Dutertre, G. Gouesbet, J. L. Hudson, and Z. Fei, J. Phys. Chem. **99**, 7016 (1995).
[4] M. Giona, F. Lentini, and V. Cimagalli, Phys. Rev. A **44**, 3496 (1991).
[5] G. Gouesbet and J. Maquet, Physica D **58**, 202 (1992).
[6] G. Gouesbet and C. Letellier, Phys. Rev. E **49**, 4955 (1994).
[7] L. A. Aguirre and S. A. Billings, Int. J. Bifurcation Chaos Appl. Sci. Eng. **5**, 449 (1995).
[8] J. L. Breeden and A. Hübler, Phys. Rev. A **42**, 5817 (1990).
[9] P. Grassberger, H. Kantz, and U. Moenig, J. Phys. A **22**, 5217 (1989).
[10] K. Ikeda, Opt. Commun. **30**, 257 (1979).
[11] C. Letellier, E. Ringuet, B. Maheu, J. Maquet, and G. Gouesbet, Entropie **202/203**, 147 (1997).
[12] W. H. Press, B. P. Flannery, S. A. Teukolsky, and W. T. Vetterling, *Numerical Recipes* (Cambridge University Press, Cambridge, 1988).
[13] E. Ott, *Chaos in Dynamical Systems* (Cambridge University Press, Cambridge, 1993).
[14] E. Lorenz, J. Atmos. Sci. **20**, 130 (1963).
[15] O. Rössler, Phys. Lett. **57A**, 397 (1976).
[16] C. Letellier, P. Dutertre, and B. Maheu, Chaos **5**, 271 (1995).
[17] J. L. Hudson and T. T. Tsotsis, Chem. Eng. Sci. **49**, 1493 (1994).
[18] F. Albahadily and M. J. Schell, J. Chem. Phys. **88**, 4312 (1988).